Catal Lett (2007) 119:346–352
DOI 10.1007/s10562-007-9242-2

Characteristics and Catalytic Properties of Pd/SiO_2 Synthesized by One-step Flame Spray Pyrolysis in Liquid-phase Hydrogenation of 1-Heptyne

Sirima Somboonthanakij · Okorn Mekasuwandumrong · Joongjai Panpranot · Tarit Nimmanwudtipong · Reto Strobel · Sotiris E. Pratsinis · Piyasan Praserthdam

Received: 10 June 2007 / Accepted: 2 August 2007 / Published online: 7 September 2007

Abstract In this study, Pd/SiO_2 catalysts with 0.5–10 wt.% Pd loadings were prepared by one-step flame spray pyrolysis (FSP) and characterized by N_2 physisorption, X-ray diffraction (XRD), transmission electron microscopy (TEM), CO chemisorption, and X-ray photoelectron spectroscopy (XPS). The average cluster/particles size of Pd as revealed by TEM were *ca.* 0.5–3 nm. The turnover frequencies (TOFs) of the flame-made catalysts decreased from 66.2 to 4.3 per s as Pd loading increased from 0.5 to 10 wt.%, suggesting that the catalytic activity was dependent on Pd particle/cluster size. However, there were no appreciable influences on 1-heptene selectivity. The flame-made Pd/SiO_2 showed better properties than the conventional prepared catalysts. Their advantages are not only the presence of large pores that facilitates diffusion of the reactants and products, but also the high-catalytic activity of as-synthesized catalysts so that further pretreatment is not necessary.

S. Somboonthanakij · J. Panpranot (✉) · T. Nimmanwudtipong · P. Praserthdam
Center of Excellence on Catalysis and Catalytic Reaction Engineering, Department of Chemical Engineering, Faculty of Engineering, Chulalongkorn University, Bangkok 10330, Thailand
e-mail: joongjai.p@eng.chula.ac.th

O. Mekasuwandumrong
Department of Chemical Engineering, Faculty of Engineering and Industrial Technology, Silpakorn University, Nakorn Pathom 73000, Thailand

R. Strobel · S. E. Pratsinis
Particle Technology Laboratory, Department of Mechanical and Process Engineering, ETH Zentrum, Swiss Federal Institute of Technology, CH-8092 Zurich, Switzerland

Keywords Flame spray pyrolysis · Pd/SiO_2 · Liquid phase hydrogenation · 1-Heptyne hydrogenation · Pd nanoparticle

1 Introduction

The selective hydrogenation of alkynes to alkenes is an important reaction in the synthesis of biologically active compounds such as insect sex pheromones (pest control) and vitamins [1]. Palladium (Pd) is the most selective of the noble metal catalysts for alkyne semihydrogenation with respect to over all alkene formation [2]. The classic Lindlar catalyst, consisting of metallic Pd on calcium carbonate support modified with lead(II) acetate, is the well known commercially available catalyst for such reaction. As reported by several authors, high activity and selectivity may be obtained over other catalyst systems in which modifiers are not necessary such as supported Pd complexes [3–5], bimetallic $Pd–Cu/SiO_2$ [6], Pd/montmorillonite [7], Pd/pumice [8], Pd/MCM-41 [9], Pd/activated carbon, and Pd/Al_2O_3 [10]. The advantages of the reaction in heterogeneous conditions are easy separation from the reaction media and possibility of continuous operation [11]. These catalyst systems, however, may require several steps during preparation such as calcination and high-temperature reduction pretreatment in order to obtain high-catalytically active components.

Flame synthesis, especially flame spray pyrolysis (FSP), is a relatively new process for one-step synthesis of supported metal catalysts. It is generally known as a method for making nanoparticles such as fume silica, titania, and carbon black in large quantity at low cost [12]. Supported metal catalysts synthesized via one-step FSP have been employed in various catalytic reactions

and they often showed improved catalytic performances [13–18]. Their differences in catalytic behaviors were suggested to be due to the structural differences of the flame-made and the conventionally prepared catalysts.

In this work, Pd/SiO_2 catalysts with 0.5–10 wt.% Pd loadings were prepared in one-step by FSP. The catalysts were characterized by N_2 physisorption, X-ray diffraction (XRD), CO pulse chemisorption, transmission electron spectroscopy (TEM), and X-ray photoelectron spectroscopy (XPS). The catalytic behaviors of the flame-made Pd/SiO_2 were evaluated in the liquid-phase selective hydrogenation of 1-heptyne under mild conditions.

2 Experimental

2.1 Catalyst Preparation

Synthesis of Pd/SiO_2 was carried out using a flame spray reactor similar to that of Ref. [19]. Palladium actetylacetonate and tetraethylorthosilicate (TEOS) from Aldrich, Tanfkirchen, Germany, were used as palladium and silicon precursors, respectively. Precursors were prepared by dissolving in xylene (MERCK, Hohenbrumn, Germany; 99.8 vol.%)/acetonitrile (Fluka, Steinheim, Germany; 99.5 vol.%) mixtures (70/30 vol.%) with total metal concentration maintained at 0.5 M. The palladium concentration was ranged between 0.5 and 10 wt.%. Using a syringe pump, 5 ml/min of precursor solution was dispersed into fine droplets by a gas-assist nozzle fed by 5 l/min of oxygen (Thai Industrial Gas Limited, Bangkok, Thailand; purity >99%). The pressure drop at the capillary tip was maintained at 1.5 bar by adjusting the orifice gap area at the nozzle. The spray was ignited by supporting flamelets fed with oxygen (3 l/min) and methane (1.5 l/min) which are positioned in a ring around the nozzle outlet. A sintered metal plate ring (8 mm wide, starting at a radius of 8 mm) provided additional 10 l/min of oxygen as sheath for the supporting flame. The product particles were collected on a glass fiber filter (Whatman GF/C, Kent, UK, 15 cm in diameter) with the aid of a vacuum pump.

For comparison purposes, 1 wt.% Pd on a commercial SiO_2 (Strem Chemicals, Newburyport, MA, USA, *specific surface area* 243.8 m^2/g V_{Pore} 1.06 m^3/g d_{Pore} 17.4 nm) was prepared by incipient wetness impregnation using $Pd(NH_3)_4Cl_2$ (Aldrich) as palladium precursor. The catalyst was dried in oven at 100 °C and calcined in air at 450 °C for 3 h. Prior to reaction, the catalyst was reduced ex situ in H_2 flow at room temperature for 2 h. Properties of the reference catalyst can be found in Ref. [20].

2.2 Catalyst Characterization

X-ray diffraction patterns were recorded with a Siemens D5000 using nickel filtered CuK_α radiation. The crystallite size (d_{XRD}) was determined using the Scherrer equation and α-alumina as the external standard. The Brunauer Emmett Teller (BET) surface area, average pore size diameters, and pore size distribution are determined by physisorption of nitrogen (N_2) using a Micromeritics ASAP 2020 automated system. The average palladium cluster/particle size and distribution of palladium on silica was observed using a JEOL-JEM 200CX transmission electron microscope operated at 100 kV. The active sites and relative percentages dispersion of palladium catalyst were determined by CO-pulse chemisorption technique using a Micromeritics ChemiSorb 2750 system attached with ChemiSoft TPx software at room temperature. XPS analysis was performed using an AMICUS photoelectron spectrometer equipped with a Mg K_α X-ray as a primary excitation and a KRATOS VISION2 software. XPS elemental spectra were acquired with 0.1 eV energy step at a pass energy of 75 kV. The C 1 s line was taken as an internal standard at 285.0 eV.

2.3 Catalytic Evaluation

The selective hydrogenation of 1-heptyne (Aldrich) was carried out in magnetically stirred 50-ml stainless steel autoclave reactor (JASCO, Tokyo, Japan). Approximately 20 mg of Pd/SiO_2 catalyst was dispersed in a 10 ml of 2% (v/v) solution of 1-heptyne (Fluka) in toluene. The reaction was carried out under ultra high-purity hydrogen atmosphere at 1 bar and 30 °C for 5 min. The liquid reactants and products were analyzed by gas chromatography equipped with an FID detector (Shimadzu GC-14A, Kyoto, Japan) and a GS-alumina (length = 30 m, I.D. = 0.53 mm) packed column.

3 Results and Discussion

3.1 Catalyst Properties

Figure 1 shows the XRD patterns of the flame-made SiO_2 and Pd/SiO_2 catalysts with Pd loadings 0.5–10 wt.%. All the catalyst samples exhibited only the characteristic peaks of amorphous silica except that of 10 wt.% Pd/SiO_2 where additional peaks corresponding to Pd^0 metal were apparent (major peak at 40.1° 2θ). It is suggested that very fine palladium metal clusters/particles were finely dispersed in the silica matrix for the catalysts with low-Pd loadings. Unlike typical supported metal catalysts prepared by wet

impregnation that calcination and reduction steps are required in order to obtain catalytically active metal surface, the flame-made supported metal catalysts can be used as synthesized and calcination/reduction step is not necessary since the metal is available in its reduced form as synthesized [14–16]. Figure 2a shows typical TEM micrographs of the flame-made Pd/SiO_2 catalysts with different Pd contents. The Pd clusters were found to be in spherical shape with average diameters *ca.* 0.5–3 nm with narrow size distribution confined to the surface of SiO_2 particles. The TEM images were quite similar to those of Pd/Al_2O_3 catalysts prepared via flame process reported by Strobel et al. [16]. However, it is surprising that for Pt/SiO_2 prepared by FSP under similar conditions using platinum acetylacetonate as Pt precursor, some very large Pt particles (>100 nm) were obtained due to incomplete evaporation [15]. This was not the case for the flame-derived Pd/SiO_2 in which only small Pd particles were observed. The average clusters sizes of palladium increased from 0.5 to 3 nm as Pd loading increased from 0.5 to 2 wt.% and remained at *ca.* 3 nm even after increasing of Pd loading to 10 wt.%.

Table 1 summarizes some physicochemical properties of the SiO_2, the flame-made Pd/SiO_2 catalysts, and the 1%Pd on commercial SiO_2. The BET surface area of the flame-made SiO_2 was 196 m^2/g whereas those of the flame-made Pd/SiO_2 catalysts were in the range of 246–306 m^2/g. The BET surface areas of the flame-made catalysts increased as Pd contents increased from 0.5 to 5 wt.% and were slightly decreased when Pd loading was increased from 5 to 10 wt.% (from 306 to 299 m^2/g). An increase in BET surface areas of the flame-made catalysts compared to the SiO_2 support was due probably to inhibition of the growth of the SiO_2 particles by Pd dopant. Such result is similar to the works reported by Hannemann et al. [21] for Au–Ag/SiO_2 nanoparticles prepared by FSP

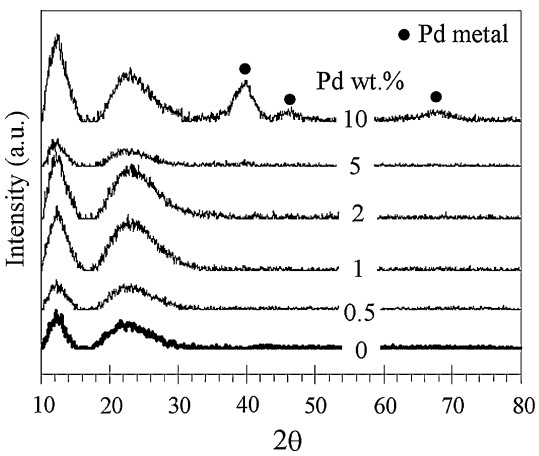

Fig. 1 XRD patterns of the flame-made Pd/SiO_2 catalysts (as synthesized)

that adding metal particles resulted in an increase in BET surface area of the SiO_2 support. Pore volumes of the flame-made catalysts also increased with increasing Pd loading and were determined to be 0.43–0.69 cm^3/g. The pore size distribution patterns of the flame-made samples as calculated by BJH desorption equation suggest the presence of mostly meso- and macro-pores (Fig. 3). The average pore diameters were unaltered for the flame-made Pd/SiO_2 catalysts with Pd loading between 0.5 and 5 wt.% while that of the 10%Pd/SiO_2 increased slightly. The presence of large pores in the flame-made catalysts can help facilitating diffusion of both reactants and products. It has been reported that diffusion limitation of reactants occurred when much smaller pore sizes of the supports were used (average pore size <10 nm) for Pd catalysts in liquid phase hydrogenation [22, 23]. These pores were larger than that of the commercial SiO_2 used in this study.

Typically, BET surface areas of supported metal catalysts are less than that of the original support due to pore blockages of metal particles during impregnation and/or calcination step. Structural difference of the flame-made catalysts suggests different mechanism for the formation of metal/metal oxide particles. Formation of Pd/SiO_2 nanoparticles by FSP was considered as follows: the sprayed droplets of precursor solution were evaporated and combusted as soon as they met the flame at very high temperature and released the metal atoms, then nucleation and growth of particles by coagulation and condensation occurred along the axial direction of the flame. Comparing to silica, the vapor pressure of Pd/PdO was higher in the hot flame environment, and consequently SiO_2 particle formation started earlier. Further downstream of the flame at lower temperatures, Pd/PdO started to form small particles which were deposited directly on the SiO_2. Similar particle formation mechanism has been suggested for Pd/Al_2O_3 and Pt/TiO_2 [16–24].

On the other hand, the 1%Pd/SiO_2-com exhibited XRD characteristic peaks of PdO at 2θ degree = 33.8, and less so at 42.0, 54.8, 60.7, and 71.4 (results not shown). The average PdO crystallite sizes calculated from the full width at half maximum of the XRD peak at $2\theta = 33.8°$ using Scherrer equation was 11.4 nm. The relative amounts of active surface Pd metal on the as-synthesized FSP-catalyst samples were calculated from CO chemisorption experiments at room temperature and are given in Table 1. It has been confirmed by CO chemisorption experiments that these FSP-derived Pd/SiO_2 catalysts with or without H_2 reduction adsorbed similar amounts of CO. Thus, it is likely that palladium were deposited on the as-synthesized Pd/SiO_2 catalysts as Pd^0 metal. The Pd active sites were then calculated based on the assumption that one carbon monoxide molecule adsorbs on one palladium site [25, 26]. The Pd active sites were found to increase from

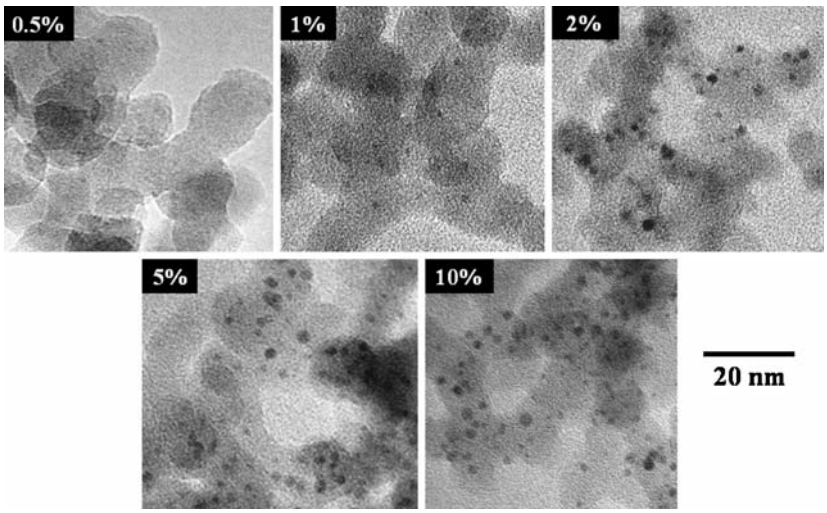

Fig. 2 TEM micrographs of (**a**) the as-synthesized and (**b**) the spent flame-made Pd/SiO_2 catalysts (after reaction)

0.97×10^{18} to 25.84×10^{18} sites/g catalyst as the Pd contents increased from 0.5 to 10 wt.% and corresponding to increasing of %Pd metal dispersion from 3.4 to 4.6%. The average Pd^0 metal particle sizes calculated from CO chemisorption were found to be in the range of 24–39 nm which were much larger than those based on XRD and TEM analyses. In general, low-metal dispersion and overestimation of metal particle sizes in supported metal catalysts based on CO chemisorption have possibly been due to (a) partial blockage of CO adsorption as a result of pore blockage by agglomeration of metal particles [27] and (b) localized destruction of the pore structure forming cracks and holes where larger metal particles could form and chemisorption would also be restricted [28], or (c) chemisorption suppression due to strong support-metal interactions [29]. In this case, low-CO chemisorption uptake of the catalysts with relatively low-metal loadings may be due to the formation of Si–O groups covering the small Pd metal clusters/particles resulting in an inhibition of CO chemisorption. Otherwise, an alloy of Pd and Si may be formed resulted in a strong interaction between Pd and SiO_2. Chemisorption suppression may relate to a decrease in the kinetics of chemisorption as a result of it becoming highly activated, therefore, resulting in poor uptake at a given temperature.

X-ray photoelectron spectroscopy is a powerful tool for determination of the surface compositions of the catalysts and the interaction between Pd and silica supports. The

Table 1 Physicochemical properties of flame-made SiO_2 and Pd/SiO_2 catalysts

Catalyst	BET surface areas[a] (m^2/g)	Pore volume[a] (cm^3/g)	CO chemisorption results[b]			XPS results Pd $3d_{5/2}$		Atomic ratio[e] (Pd/Si)
			CO uptake ($\times 10^{-18}$ molecule CO/g cat.)	%Pd dispersion[c]	$d_PPd^{0,d}$ (nm)	B.E. (eV)	FWHM	
SiO_2	196	0.48	n/a[f]	n/a	n/a	n/a	n/a	n/a
0.5%Pd/SiO_2	246	0.43	1.0	3.42	33	n/a	n/a	0.0011
0.5%Pd/SiO_2_R[g]	–	–	1.1	3.53	32	–	–	–
1%Pd/SiO_2	251	0.46	1.9	3.40	33	n/a	n/a	0.0014
2%Pd/SiO_2	260	0.49	3.3	2.88	39	n/a	n/a	0.0018
5%Pd/SiO_2	306	0.59	13.4	4.71	24	337.4	2.389	0.0139
10%Pd/SiO_2	299	0.69	25.8	4.55	25	337.4	3.189	0.0404
1%Pd/SiO_2-com	234	1.02	3.3	5.81	19	–	–	0.0033

[a] Error of measurement was ± 10%

[b] Error of measurement was ± 5% as determined directly

[c] Based on the total palladium loaded and an assumption of CO/Pd = 1

[d] Based on $d = (1.12/D)$ nm [25], where D = fractional metal dispersion

[e] Based on XPS results

[f] n/a = not available

[g] R = after reduced for 2 h in H_2 at room temperature

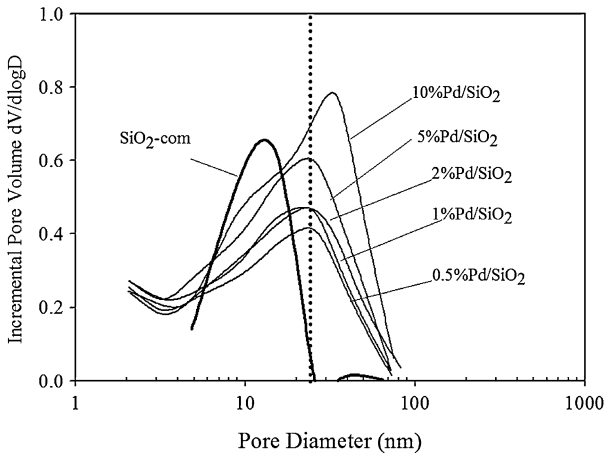

Fig. 3 Pore size distribution of the flame-made Pd/SiO_2 catalysts with 0.5–10 wt.% Pd loading

elemental scans for Pd $3d_{5/2}$ of the various flame-made Pd/SiO_2 catalysts are shown in Fig. 4. No distinctive peaks for Pd $3d_{5/2}$ were observed for the flame-made Pd/SiO_2 with Pd loading between 0.5 and 2 wt.% suggesting that very low amount of Pd present on the catalyst surface. The binding energies of Pd $3d_{5/2}$ for the 5 and 10 wt.% Pd/SiO_2 were 337.4 eV which was 0.2 eV higher than Pd $3d_{5/2}$ on the classic Lindlar catalysts according to the literature [2]. It was also 2.3 eV higher than that corresponding to Pd^0 (335.1 eV) [30], which indicating that Pd in the flame-made Pd/SiO_2 catalyst is electron-deficient. The FWHM values, higher than 2.0 eV, are also indicative that more than one Pd species may be present in the flame-made Pd/SiO_2 as have been suggested for Pd/Al_2O_3 and Pd/C catalysts prepared by conventional impregnation technique [31]. The percentages of atomic concentration for Si 2p, O 1 s, and Pd 3d are also given in Table 1. For the catalysts with Pd loading 0.5–2 wt.%, much lower Pd/Si ratios were observed compared to those with higher Pd loadings (5–10 wt.%). Such results are in good agreement with the CO chemisorption results that for the catalysts with relative low-metal loadings, the metal surface may be covered by Si–O groups due to simultaneous crystallization of Pd and SiO_2 in gas-phase during FSP. It is also possible that some of the Pd metal surfaces were partially oxidized, while the kernel of the Pd particles is metallic. This would also explain the broad and not very intense XPS lines.

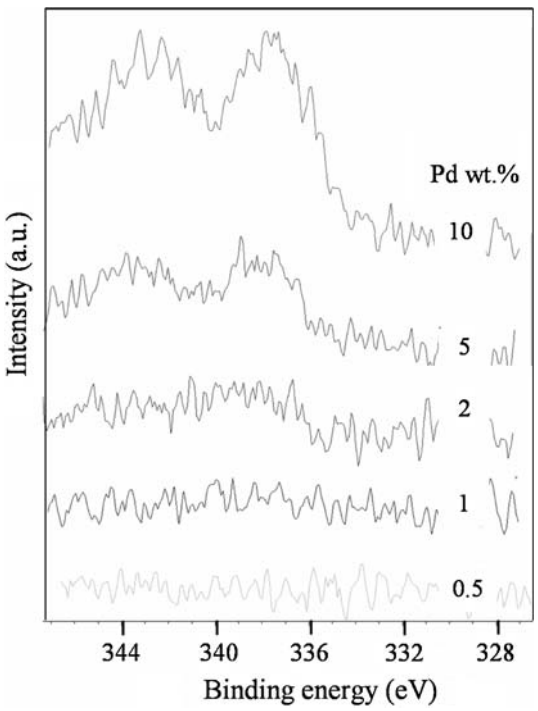

Fig. 4 XPS results for Pd $3d_{5/2}$ of the flame-made Pd/SiO_2 catalysts

3.2 Selective Hydrogenation of 1-Heptyne

The catalytic behavior of the flame-made Pd/SiO_2 catalysts was investigated in the liquid-phase selective hydrogenation of 1-heptyne in a batch system. High-stirring rate (1,000 rpm) was used in order to ensure that the reaction rate does not depend on the external mass transfer of hydrogen. However, it should be noted that external mass transfer control may still exist if the relative velocity between fluid and particles is close to zero. As mentioned earlier, the average pore sizes of all the flame-made Pd/SiO_2 catalysts were much larger than those reported in the literature in which diffusion limitation of reactants occurred (usually average pore size of the supports <10 nm), therefore, the effect of pore size on the reaction rate could be negligible in this study. The catalytic performance in terms of 1-heptyne conversions and selectivities to 1-heptene and the turnover frequencies (TOFs) calculated based on CO chemisorption results of the flame-made Pd/SiO_2 catalysts are given in Table 2. The conversion of 1-heptyne increased from 42 to 75% as Pd loading increased from 0.5 to 5 wt.% and remained relatively constant when Pd loading was increased to 10 wt.%. The selectivities for 1-heptene were in the range of 92–95% for all the Pd/SiO_2 catalysts. Based on the conditions and the column used in our GC analysis, the other product found in the reaction besides 1-heptene is *n*-heptane. No other by-products were observed. For similar Pd loading, the catalytic activity of the flame-made catalyst was considerably higher than that of Pd/SiO_2 catalyst prepared by incipient wetness impregnation on a commercial SiO_2 support. The results of this study follow the trend in the literature that alkyne hydrogenation activity of Pd catalyst depends largely on Pd dispersion and there is no appreciable influence on

Table 2 Catalytic properties for liquid-phase 1-heptyne selective hydrogenation

Catalyst	Conversion (%)	1-Heptene selective (%)	TOF[a] (s^{-1})
0.5%Pd/SiO_2	42	93	66.2
1%Pd/SiO_2	43	92	34.1
	100[b]	62[b]	–
2%Pd/SiO_2	54	94	25.3
5%Pd/SiO_2	75	95	8.6
10%Pd/SiO_2	73	94	4.3
1%Pd/SiO_2-com	20	100	7.7
	100[b]	13[b]	–

Reaction conditions were 105 kPa, 30 °C, 5 min, and catalyst/substrate molar ratio = 1/1,600

[a] TOF = mole product/mole Pd metal/s. Based on the amount of active Pd atoms measured by CO chemisorption

[b] Reaction conditions were 105 kPa, 30 °C, 40 min, and catalyst/substrate molar ratio = 1/500

alkene selectivity [32, 33]. In general, 1-heptene selectivity decreases with increasing 1-heptyne conversion. Under similar reaction conditions, the flame-derived catalysts exhibited higher 1-heptyne conversion than the impregnated ones and slightly lower 1-heptene selectivity. However, at 100% conversion of 1-heptyne, the selectivities for 1-heptene for the flame-made and the impregnated catalysts were 62 and 13%, respectively. The specific activities of the flame-made catalysts are also expressed in terms of TOF which is defined as mole of product/mole of metal/time. As the palladium loading increased from 0.5 to 10 wt.%, the TOFs of the flame-made catalysts decreased from 66.2 to 4.3 per s. Much higher TOFs values for the catalysts with relatively low-metal loadings (≤2 wt.%) are another evidence that CO chemisorption suppression occurred on these catalysts. It was probably due to the formation of very fine palladium metal clusters/particles or an alloy of Pd and Si which resulted in a strong interaction between Pd and SiO_2. Moreover, formation of Si–O groups at the metal surface due to homogeneous crystallization of Pd^0 and SiO_2 in gas phase during flame spray synthesis or partially oxidized Pd at the surface could also result in the inhibition of CO chemisorption. For the 10 wt.% Pd/SiO_2, there was probably no CO chemisorption suppression since most of the Pd was in metallic state as indicated by XRD so the TOFs still decreased from 2 to 10 wt.% Pd loadings in spite of similar particle size of these catalysts. The remarkable high-catalytic hydrogenation activities (TOFs) of Pd nanoparticles, however, have also been reported for other Pd/SiO_2 systems [34–36]. The durability of the catalysts under repeated catalytic cycles was tested on both the flame-made 1%Pd/SiO_2 and 1%Pd/SiO_2-com catalysts. After different numbers of reaction cycles (0, 1, 2, or 3), the used catalyst was filtered out and dried at room temperature before being re-used in the reaction. It was found that the catalytic activity decreased by *ca.* 50 and 30% after the third cycle of run, respectively. Such results suggest that catalyst deactivation is still a problem in the liquid-phase reaction.

4 Conclusions

Flame spray pyrolysis is an effective method for one-step synthesis of Pd nanoparticles with average size of 0.5–3 nm on SiO_2 supports. The as-synthesized FSP-derived catalysts showed higher catalytic activities for selective hydrogenation of 1-heptyne under mild conditions than the conventional prepared Pd/SiO_2 catalyst. The TOFs of the flame-made Pd/SiO_2 decreased with increasing Pd particle/cluster size suggesting that alkyne hydrogenation activity depends on Pd dispersion. However, there is no appreciable influence on alkene selectivity.

Acknowledgments The authors would like to thank the financial supports from the Graduate School of Chulalongkorn University (the 90th Anniversary of Chulalongkorn University-the Golden Jubilee Fund), the Thailand Research Fund (TRF), the National Science and Technology Development Agency (NSTDA), and the Research and Development Institute of Silpakorn University.

References

1. Bailey S, King F (2000) In: Sheldon RA, van Bekkum H (eds) Fine chemicals through heterogeneous catalysis, Chap. 8. Wiley-VCH, Germany
2. Marin-Astorga N, Alvez-Manoli G, Reyes P (2005) J Mol Catal A 226:81
3. L'Argentiere PC, Cagnola EA, Quiroga ME, Liprandi DA (2002) Appl Catal A 226:253
4. Cagnola E, Liprandi D, Quiroga M, L'Argentiere P (2003) React Kinet Catal Lett 80:277
5. L'Argentiere PC, Quiroga ME, Liprandi DA, Cagnola EA, Roman-Martinez MC, Diaz-Aunon JA, Salinas-Martinez de Lecea C (2003) Catal Lett 87:97
6. Nijhuis TA, van Koten G, Moulijn JA (2003) Appl Catal A 238:259
7. Mastalir A, Kiraly Z, Szollosi G, Bartok M (2000) J Catal 194:146
8. Gruttadauria M, Liotta LF, Noto R, Deganello G (2001) Tetrahedron Lett 42:2015
9. Marin-Astorga N, Pecchi G, Fierro JLG, Reyes P (2003) Catal Lett 91:115
10. Lederhos CR, L'Argentiere PC, Figoli NS (2005) Ind Eng Chem Res 44:1752
11. Lennon D, Marshall R, Webb R, Jackson SD (2000) Stud Surf Sci Catal 130:245
12. Stark WJ, Pratsinis SE (2002) Powder Technol 126:103
13. Piacentini M, Strobel R, Maciejewski M, Pratsinis SE, Baiker A (2006) J Catal 243:43
14. Strobel R, Krumeich F, Pratsinis SE, Baiker A (2006) J Catal 243:229

15. Height MJ, Pratsinis SE, Mekasuwandunrong O, Praserthdam P (2006) Appl Catal B 63:305
16. Strobel R, Stark WJ, Madler L, Pratsinis SE, Baiker A (2003) J Catal 213:296
17. Strobel R, Krumeich F, Stark WJ, Pratsinis SE, Baiker A (2004) J Catal 222:307
18. Hannemann S, Grunwaldt J-D, Lienemann P, Gunther D, Krumeich F, Pratsinis SE, Baiker A (2007) Appl Catal A 316:226
19. Mädler L, Stark WJ, Pratsinis SE (2002) J Mater Res 17:1356
20. Panpranot J, Phandinthong K, Sirikajorn T, Arai M, Praserthdam P (2007) J Mol Catal A 261:29
21. Hannemann S, Grunwaldt J, Krumeich F, Kappen P, Baiker A (2006) Appl Surf Sci 52:7862
22. Sato S, Takahashi R, Sodesawa T, Koubata M (2005) Appl Catal A 284:247
23. Mastalir A, Rac B, Kiraly Z, Molnar A (2007) J Mol Catal A 264:170
24. Teoh WY, Mädler L, Beydoun D, Pratsinis SE, Amal R (2005) Chem Eng Sci 60:5852
25. Mahata N, Vishwanathan V (2000) J Catal 196:262
26. Ali SH, Goodwin JG Jr (1998) J Catal 176:3
27. Verdonck JJ, Jacobs PA, Genet M, Poncelet G (1980) J Chem Soc Faraday Trans 76:403
28. Gustafson BL, Lunsford JH (1982) J Catal 74:393
29. Tauster S J, Fung SC, Garten RL (1978) J Am Chem Soc 100:170
30. Wagner CD, Riggs WM, Davis LE, Moulder JF (1978) In: Muilenberg GE (ed) Handbook of X-ray photoelectron spectroscopy. Perkin-Elmer Corporation, Eden Prairie, MN
31. Lederhos RC, L'Argentiere PC, Fıgoli NS (2005) Ind Eng Chem Res 44:1752
32. Papp A, Molnar A, Mastalir A (2005) Appl Catal A 289:256
33. Mastalir A, Kiraly Z (2003) J Catal 220:372
34. Dominguez-Quintero O, Martinez S, Henriquez Y, D'Ornelas L, Krentzien H, Osuna J (2003) J Mol Catal A 197:185
35. Mu X, Bartmann U, Guraya M, Busser GW, Weckenmann U, Fischer R, Muhler M (2003) Appl Catal 248:85
36. Kim N, Kwon MS, Park CM, Park J (2004) Tetrahedron Lett 45:7057